

UNCLASSIFIED

Copy 6
RM L56G31



~~CONFIDENTIAL~~

UNCLASSIFIED

0.2

NACA RM L56G



RESEARCH MEMORANDUM

WIND-TUNNEL MEASUREMENTS OF WING BUFFETING ON 1/16-SCALE
MODEL OF DOUGLAS D-558-II RESEARCH AIRPLANE

By William B. Kemp, Jr., and Thomas J. King, Jr.

Langley Aeronautical Laboratory
Langley Field, Va.

LIBRARY COPY

SEP 28 1956

LANGLEY AERONAUTICAL LABORATORY
LIBRARY NACA
LANGLEY FIELD, VIRGINIA

CLASSIFIED DOCUMENT

This material contains information affecting the National Defense of the United States within the meaning of the espionage laws, Title 18, U.S.C., Secs. 793 and 794, the transmission or revelation of which in any manner to an unauthorized person is prohibited by law.

NATIONAL ADVISORY COMMITTEE FOR AERONAUTICS

WASHINGTON

September 24, 1956

*naca
BY AUTHORITY OF
RA-129. Effective 7/17/58
JSH*

UNCLASSIFIED

~~CONFIDENTIAL~~

NATIONAL ADVISORY COMMITTEE FOR AERONAUTICS

RESEARCH MEMORANDUM

WIND-TUNNEL MEASUREMENTS OF WING BUFFETING ON 1/16-SCALE
MODEL OF DOUGLAS D-558-II RESEARCH AIRPLANE

By William B. Kemp, Jr., and Thomas J. King, Jr.

SUMMARY

Exploratory measurements have been made of the fluctuations of wing bending moment during normal performance and stability wind-tunnel tests of a model of the Douglas D-558-II research airplane at Mach numbers from 0.60 to 0.96. The effects of leading-edge chord-extensions and several pylon-mounted underwing external stores were investigated.

Analysis of the measurements indicated that the standard deviation of the wing bending moment was a qualitative indication of buffeting intensity. Quantitative application of the measurements was limited by model response in vibration modes having no counterpart in flight and by possible effects of model structural damping.

The addition of leading-edge chord-extensions caused practically no change in the buffet boundary but caused an appreciable increase in model buffeting response at angles of attack well above the buffet boundary. The addition of any of the external stores caused only small changes in model buffeting response at positive angles of attack but caused noticeable increases in response at negative angles of attack. This comparison might be influenced by the effect of store mass on the frequency and shape of the model vibration modes. The horizontal tail did not contribute significantly to the buffeting response measured on the wing.

INTRODUCTION

In order to give due consideration to the phenomenon of buffeting in the preliminary stages of aircraft design, the designer must have information on the effects of many types of changes in aircraft configuration on the extent of the flight regime in which buffeting is encountered and on the magnitude of the buffeting loads. The task of providing this information would appear much simpler to perform in a wind tunnel than in flight tests if a method of obtaining quantitative buffeting measurements

on a wind-tunnel model were available. The amplitude of fluctuation of the wing root bending moment was selected as a parameter which would indicate the presence and magnitude of buffeting on a conventional wind-tunnel model with some hope of quantitative application to flight conditions.

In order to study the behavior of this parameter, some exploratory measurements of fluctuations of wing root bending moment were made in December 1953 during conventional drag and stability tests of a model of the Douglas D-558-II research airplane. The measurements were made at high subsonic speeds with the model in the clean configuration, with leading-edge chord-extensions, and with several underwing-external-store configurations. It should be emphasized that measurement of the bending-moment fluctuations was considered a secondary purpose of these tests and, consequently, neither the model design nor the test program were influenced by consideration of the fluctuation measurements. The drag and stability results of these tests are reported in reference 1.

In reference 2 the suggestion was made that buffeting be considered the linear response of an aerodynamically damped elastic system to an aerodynamic excitation which is a stationary random process. This concept was extended in reference 3 to the development of scaling relations which were used in a brief correlation of wind-tunnel and flight buffeting measurements on two airplanes. Some of the wind-tunnel measurements used were taken from the investigation reported in this paper.

The work of reference 3 establishes the significance of wind-tunnel buffeting measurements such as those made on the D-558-II model. The present paper was prepared, therefore, to report all the buffeting measurements made during the wind-tunnel tests of the D-558-II model and to discuss the interpretation of these measurements in the light of current knowledge about buffeting.

SYMBOLS

b	wing span, ft
c	local wing chord parallel to free stream, ft
\bar{c}	mean aerodynamic chord of wing, $\frac{2}{S} \int_0^{b/2} c^2 dy$, ft
C_D	drag coefficient, $\frac{\text{Drag}}{qS}$
C_L	lift coefficient, $\frac{\text{Lift}}{qS}$

C_m	pitching-moment coefficient, $\frac{\text{Pitching moment}}{qS\bar{c}}$
C_N	normal-force coefficient, $\frac{\text{Normal force}}{qS}$
i_t	horizontal tail incidence from fuselage reference line, deg
M	Mach number
p	free-stream static pressure, lb/sq ft
q	free-stream dynamic pressure, $\frac{1}{2}\rho V^2$, lb/sq ft
R	Reynolds number, based on wing mean aerodynamic chord
S	wing area, sq ft
T_t	stagnation temperature, °F
V	free-stream velocity, ft/sec
α	angle of attack of fuselage reference line, deg
ΔC_N	incremental fluctuation of airplane normal-force coefficient due to buffeting
ρ	mass density of air, slugs/cu ft
σ_b	standard deviation of wing bending moment (root-mean-square deviation from the mean), in-lb

DESCRIPTION OF MODEL

A three-view drawing of the model giving the basic geometric characteristics is presented in figure 1. Photographs showing the model installed in the Langley high-speed 7- by 10-foot tunnel in the clean configuration and with one arrangement of external stores are presented in figures 2(a) and 2(b), respectively. There were some differences between the model and the Douglas D-558-II airplane which included an enlarged rearward portion of the model fuselage to allow attachment of a sting support and a model wing-tip thickness ratio of 10 percent instead of 12 percent. The model did not include the wing fences normally used on the airplane.

~~CONFIDENTIAL~~

The model components were machined from solid duralumin with the exception of the steel fuselage nose, wooden canopy, and brass vertical tail. Each wing panel and an appreciable portion of the fuselage midsection were machined as a unit. The bolted connections between these parts and the remainder of the fuselage were so designed that the structure between the wing panels was highly rigid and presented little opportunity for relative motion between parts.

Figure 3 gives dimensions of the leading-edge chord-extensions which were installed for some tests. Details of the external stores investigated are presented in figure 4. Each store installation consisted of two identical stores located symmetrically from the plane of symmetry at 0.61 semispan. The stores were of two different shapes (ordinates in table I) that were scaled to produce three sizes of one shape (designated stores A, B, and C) and one size of the other (designated store D). The shape of stores A, B, and C, which will be referred to as the short-cylinder shape, is that developed by the Douglas Aircraft Company, Inc., and is frequently referred to as the DAC store shape. The shape of store D, which will be called the long-cylinder shape, was developed by the Wright Air Development Center and is frequently referred to as the WADC store shape. The stores and the store fins using the short-cylinder shape are 1/16-scale models of a full-scale 1,000-pound bomb (store A), a 2,000-pound bomb (store B), and a 150-gallon fuel tank (store C). The long-cylinder store (store D) had the same length and fin dimensions as store A; but, because of a somewhat larger diameter and different profile development, the long-cylinder shape had a greater volume.

The details of the pylons investigated are presented in figure 5. The pylons were identical in sweep and chord length, but differed in cross-section profile. The pylons are identified by their streamwise thickness ratios as the 7.6-percent pylon, the 6.2-percent pylon, and the 4.2-percent pylon. All the pylons had midchord sections with parallel sides. The 7.6-percent pylon had a shorter midchord section than either the 6.2- or the 4.2-percent pylons. The thickness distributions of the 6.2- and 4.2-percent pylons differed only by a constant factor. Ordinates of the pylons are given in figure 5. The stores and the pylons were made of solid brass.

The model was mounted on a six-component strain-gage balance located within the fuselage. The model-balance combination was supported by a sting mounting system (fig. 2) that attached to the balance through the base of the fuselage.

The following weights of the various model components were tabulated:

Component	Weight, lb
Fuselage and tail surfaces	27.83
Strain-gage balance	4.81
One wing panel (exposed)	1.12
One store A	.83
One store B	1.77
One store C	2.89
One store D	1.16
One 7.6-percent pylon	.23
One 6.2-percent pylon	.24
One 4.2-percent pylon	.16

The natural frequencies of several of the major vibration modes of the model and support system were measured for the clean model without stores or leading-edge chord-extensions. These measurements were made with the model, balance, and sting attached to a support system having different elastic properties from the support system in the tunnel. In particular the vertical stiffness of the tunnel support was greater than that of the support used for the frequency measurements. The measured natural frequency of the vertical sting bending mode was 11 cps. It is estimated that the natural frequency of this mode with the tunnel support system was of the order of 15 cps. The following measured natural frequencies tabulated for other vibration modes were probably not appreciably affected by the difference in sting-support elasticity:

Mode	Natural frequency, cps
Rigid body pitching	34
Rigid body yawing	35
Rigid body rolling	81
First wing bending	196
Second wing bending	281

The rigid-body modes were predominantly associated with balance elasticity.

INSTRUMENTATION AND TESTS

The instrumentation used for measurement of the static aerodynamic forces and moments was conventional. A six-component internal strain-gage

balance was connected to the balance readout system usually used for static tests in this tunnel.

For the buffeting measurements, strain gages were installed in shallow pockets machined in the upper and lower surfaces of each wing at the location shown in figure 3. The two gages on each wing formed the two active arms of a bridge capable of sensing wing bending moment about an axis approximately normal to the 50-percent-chord line. The output of each bridge was fed into an amplifier which eliminated the direct-current component of the signal and had a response which was flat within ± 1 percent from 10 to 2,000 cps and within ± 5 percent from 5 to 5,000 cps. The root-mean-square value (standard deviation) of the resulting signals were measured with thermocouple meters. A qualitative indication of the time constant of the thermocouple meters is obtained from the observation that after application of a constant amplitude input signal, about 10 seconds were required to obtain a steady reading. The amplifier-thermocouple-meter combinations were calibrated by using 20-cps and 100-cps alternating-voltage inputs. The calibrations were found to be independent of frequency. The strain gages, however, were calibrated with only static loadings and the calibrations thus obtained were assumed to apply to the dynamic buffeting loads. The strain-gage calibrations indicated that the actual bending-moment axis was normal to a line having about 4° greater sweep angle than the 50-percent-chord line.

For some test conditions, oscillograph records were made of the time history of the strain-gage outputs. The frequency response of the recorder was approximately flat below 500 cps. No calibration of the relation between wing bending moment and oscillograph displacement was made.

The tests were made in the Langley high-speed 7- by 10-foot tunnel at Mach numbers from 0.60 to 0.96. This tunnel is a closed return type with a closed test section and operates at essentially atmospheric stagnation pressure. The tunnel is cooled by an air exchange system. A series of four fine-mesh turbulence-damping screens are installed in the settling chamber ahead of the entrance cone. Representative values of static pressure, dynamic pressure, stagnation temperature, velocity, and Reynolds number are given for each test Mach number in table II.

RESULTS AND DISCUSSION

General Nature of Buffeting Measurements

An example of the data obtained from the wing-bending-moment gages is shown in figure 6. The standard deviation of the wing bending moment is plotted against angle of attack for the complete model without stores

or chord-extensions at a series of Mach numbers. Measurements from both wing panels are plotted on the same axes.

Each reading was made by visually averaging the indication of the thermocouple meter over a period of several seconds. The readings for the two panels were made in sequence rather than simultaneously. Even so, the point-to-point trends of the bending-moment fluctuations are remarkably similar for the two panels. This fact apparently indicates that the buffeting process was sufficiently stationary and that the data sample made use of by the instrumentation was sufficiently long for the readings to be fairly reliable indications of the magnitude of the bending-moment fluctuations. Some consistency is apparent in the small differences between the readings for the two panels which could have been produced by asymmetry in the model structural characteristics or by inaccuracies in calibration of the strain gages or associated circuits.

The variations of bending-moment fluctuations with angle of attack plotted in figure 6 are characterized by a region of small fluctuations at low angles of attack, a region of rapidly increasing fluctuations at moderate angles of attack, and a region of large fluctuations at high angles of attack. The fluctuations at low angle of attack are probably not associated with buffeting and may be attributed to airstream roughness and stray electrical and vibrational pickup in the strain-gage wiring and amplifier circuits.

At moderate and high angles of attack, the large values of fluctuations of wing bending moment undoubtedly originated primarily on the model and are therefore an indication of the model response to buffeting. The contribution of airstream roughness and stray pickup to the bending-moment fluctuations at high angles of attack is judged to be of minor importance in view of the low level of fluctuations measured at low angles of attack. Of course, the existence of these fluctuations at low angles of attack, in even the small degree present in these tests, lends difficulty to the determination of the angle of attack for onset of buffeting or buffet boundary. For these tests, the buffet boundary will be considered to be the point at which the bending-moment fluctuations begin to increase from their low angle-of-attack level. This point is probably somewhat higher than the actual buffet onset boundary which would be determined in smooth air.

Comparison of the buffeting measurements in figure 6 with the lift curves reproduced from reference 1 in figure 7 indicates that the initial buffeting was observed at about the angle of attack corresponding to the initial reduction in lift-curve slope. This result is consistent since both buffeting and reduction of lift-curve slope would be expected to result from flow separation on the wing.

The normal-force coefficient corresponding to the buffet boundary is compared in figure 8 with flight-determined buffet boundaries for the D-558-II airplane published in references 4 and 5. The model buffet boundary appears to be too low at the lower speeds and too high at Mach numbers between 0.85 and 0.95. Possible contributions to these discrepancies include differences in Reynolds number and wing-tip airfoil thickness between the model and airplane. Another contribution may be the lag in establishment of or recovery from separated flow in the fairly rapid maneuvers from which some of the flight data were obtained.

Frequency Distribution of Buffeting Response

An examination of the frequency distribution of the model response to buffeting excitation can provide additional information about the nature of the fluctuation measurements. Reference 6 outlines a numerical procedure for obtaining the power spectrum corresponding to an experimental time history. This procedure has been applied to the oscillograph records of the bending moment of the left wing of the D-558-II model obtained at several angles of attack at $M = 0.9$. The resulting power spectra are presented in figure 9 and indicated by the solid curves. The power spectral density has units of (Bending moment)²/cps but is plotted to an arbitrary scale because the calibration of the oscillograph was unknown. Comparable scales are used, however, for the four angles of attack.

The time scale of the records was such that the maximum frequency resolvable by the numerical procedure was 200 cps. Inasmuch as the measured natural frequency of the first wing bending mode was 196 cps, the frequency analyses should be interpreted with caution. One interesting feature of the analysis procedure is that the ordinate of the power spectrum at frequency f represents the sum of the power spectral densities actually existing at the frequencies $2nf_0 \pm f$ where n is zero or any positive integer and f_0 is the maximum resolvable frequency (200 cps in this case). Thus, the actual power spectrum is folded back and forth on itself so that it is wholly contained in the frequency range from 0 to 200 cps. Use was made of this feature to arbitrarily unfold the power spectra at frequencies above about 185 cps so that a more realistic appearing resonance peak would occur near 196 cps. The power spectra so adjusted are indicated by the dashed curves in figure 9. The area under each spectrum has not been changed by this process and is a measure of the square of the standard deviation of the original time history.

The power spectra for angles of attack of 4.8° , 6.9° , and 15.3° show that almost all of the buffeting response occurred in three sharply defined frequency bands with peaks at 0, 77, and 196 cps. The peak at 196 cps has significantly more area than the others and, of course, represents

the response in the first symmetrical wing bending mode. The peak at 77 cps probably represents the response in the rigid-body rolling mode with elastic restraint provided by the sting and balance. The measured natural frequency of this mode was 81 cps.

The response at very low frequencies is not so easily explained. It is interesting to note that the spectrum at $\alpha = 2.6^\circ$ which was considered below the buffet boundary shows as much very low frequency response as that at $\alpha = 4.8^\circ$ even though insignificant buffeting is indicated by the lack of response at 77 or 196 cps. The peaks at 60 and 120 cps undoubtedly result from spurious pickup of a distorted 60-cps signal from the laboratory electrical power wiring. The very low frequency response cannot be associated with any structural resonance because the lowest frequency structural mode was of the order of 15 cps. It is probable that airstream angularity fluctuations and low-frequency components of buffeting as well as stray pickup and distortion occurring during recording, reproducing, reading, and analyzing the oscillograph time histories contributed to the very low frequency portions of the spectra.

Before leaving the discussion of the power spectra, consideration should be given to the possibility of model response in modes having frequencies greater than 200 cps. Because of the aforementioned folding characteristic of the frequency-analysis procedure, any significant peak above 200 cps in the recorded signal would appear as a peak in the frequency range covered. Examination of figure 9 shows that, with the possible exception of the spectrum for $\alpha = 15.3^\circ$, the only peaks representing appreciable power are the ones previously discussed. A possible explanation is found in the power spectra of aerodynamic buffeting excitation presented in reference 7. These results show that the aerodynamic excitation falls off rapidly at values of reduced frequency above 0.5 to 1.0.

Interpretation of Model Buffeting Measurements

In reference 3, expressions are presented for scaling buffeting loads measured on a wind-tunnel model up to flight conditions. These expressions were applied in reference 3 to a comparison between measurements of buffeting loads on the D-558-II airplane in flight and some of the measurements reported in this paper. The correlation achieved by the scaling relations was promising but certain apparently systematic differences were evident between the scaled model loads and the flight loads.

One assumption used in deriving the scaling expressions of reference 3 was that the response to buffeting of the airplane structure could be treated as though it occurred entirely in the first symmetrical wing bending mode. Examination of the frequency distribution of buffeting response obtained on several airplanes in flight showed that this assumption was well justified. The spectra of the model buffeting response in

figure 9, however, show considerable response at very low frequencies and also at the frequency of the rigid-body rolling mode which has no counterpart in flight. In view of the additional model response at frequencies other than that of the first wing bending mode, it is logical to expect that the tunnel measurements scaled to flight conditions would indicate greater buffeting intensity than the corresponding flight measurements. This expectation was borne out by the comparison given in reference 3.

A second assumption used in deriving the scaling expressions was that the structural damping was negligible relative to the aerodynamic damping. This assumption also was justified by analysis of buffeting measurements made in flight but might possibly be in error for some wind-tunnel models. Although the effects of structural damping on the measurements reported in this paper cannot be isolated, some recent wind-tunnel buffeting results obtained in the Langley 8-foot transonic pressure tunnel, have indicated that the effect of structural damping on the intensity of buffeting response might have some significance for the particular model used in that investigation. Generally speaking, the effect of structural damping would become greater as the ratio of model density to air density was increased.

In view of the limitations discussed previously, the measurements reported in this paper have not been converted to dimensionless form by means of the scaling relations. Consideration of the frequency spectra presented and of the type of model construction used, however, leads to the belief that the fluctuations of the wing bending moment can be considered a qualitative indication of airplane buffeting loads.

Effects of Changes in Model Configuration

Figure 10 presents a comparison of the buffeting response measured during three test runs in the clean configuration and one test run with chord-extensions. Each curve represents a faired average of data obtained on the right and left wings. The first two runs with the clean configuration were made near the beginning of the test program, and the third was made after all the store configurations had been tested. The data of figures 6, 7, 8, and 9 were obtained from the first run.

With several exceptions, the results of the three runs with the clean configuration are in fairly good agreement. At Mach numbers of 0.85 and 0.90 considerable disagreement is apparent in a limited angle-of-attack range immediately following the initial rapid increase in buffet response. Apparently, the pattern of flow separation was critically affected by changes in surface roughness or other minor differences in this range of Mach number and angle of attack. At a Mach number of 0.96, the second run is in serious disagreement with the others at angles

of attack greater than 5° . It is possible that the proximity to tunnel choking conditions, combined with the effects of humidity and inaccuracy in setting tunnel speed, tended to stabilize the shock pattern in this particular run.

The effect of adding chord-extensions was to increase the buffeting response at angles of attack well above that for initial buffeting. The chord-extensions had very little effect on the angle of attack for initial buffeting or on the initial rate of increase of buffeting response except at a Mach number of 0.85 where the rate of increase was considerably steepened.

Inasmuch as the static characteristics obtained with chord-extensions were not included in reference 1, these characteristics are presented in figure 11 for the sake of completeness.

The buffeting results obtained at two Mach numbers for the model with external stores are presented in figures 12, 13, and 14 which show the effects of store size, store shape, and pylon thickness, respectively. Data from the second run with the clean configuration are included in these figures to represent average buffeting response for the clean configuration at these two Mach numbers. It is apparent that in the positive angle-of-attack range the addition of any of the stores to the model caused relatively small changes in buffeting response, and these changes could be either positive or negative. All the stores, however, produced a marked increase in buffeting at the most negative angle of attack tested.

In view of the relatively small overall effects of store installation, a detailed analysis of the effects of changes in store configuration will not be made. Such an analysis would require consideration of the changes in frequency and mode shapes of the wing bending mode and the rigid-body rolling mode, as well as changes in the aerodynamic excitation.

A comparison is presented in figure 15 of the buffeting response measured with two values of horizontal-tail incidence and with the horizontal tail removed. Essentially identical results were obtained with the tail off and with $i_t = -2^\circ$. With $i_t = 0^\circ$, slightly lower values of buffeting response were generally obtained at the angles of attack for which buffeting occurred. Although it is difficult to believe that installation of the horizontal tail at zero incidence actually caused a decrease in buffeting intensity from the tail-off case, it is probably safe to conclude that the amount of tail buffeting sensed by the wing-bending-moment strain gages was insignificant.

~~CONFIDENTIAL~~

CONCLUDING REMARKS

Exploratory measurements of the fluctuation of wing bending moment were made during normal performance and stability wind-tunnel tests of a model of the Douglas D-558-II research airplane. Measurements were made with the model in the clean configuration and with the addition of leading-edge chord-extensions and several configurations of external stores. The standard deviation, or root-mean-square deviation from the mean, of the wing bending moment could be interpreted as a qualitative indication of buffeting intensity. Quantitative use of this parameter as an indication of airplane buffeting was limited by model response in vibration modes having no counterpart in flight and by possible effects of model structural damping.

The addition of leading-edge chord-extensions caused practically no change in the buffet boundary but caused an appreciable increase in model buffeting response at angles of attack well above the buffet boundary. The addition of any of several underwing pylon-mounted external stores caused only small changes in model buffeting response at positive angles of attack but caused noticeable increases in response at negative angles of attack. This comparison might be influenced by the effect of store mass on the frequency and shape of the model vibration modes. The horizontal tail did not contribute significantly to the buffeting response measured on the wing.

Langley Aeronautical Laboratory,
National Advisory Committee for Aeronautics,
Langley Field, Va., July 17, 1956.

REFERENCES

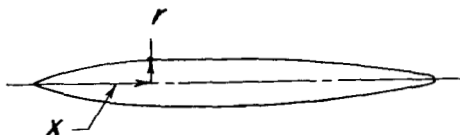
1. Silvers, H. Norman, and King, Thomas J., Jr.: Investigation at High Subsonic Speeds of the Effects of Various Underwing External-Store Arrangements on the Aerodynamic Characteristics of a 1/16-Scale Model of the Douglas D-558-II Research Airplane. NACA RM L55D11, 1955.
2. Huston, Wilber B., and Skopinski, T. H.: Measurement and Analysis of Wing and Tail Buffeting Loads on a Fighter Airplane. NACA Rep. 1219, 1955. (Supersedes NACA TN 3080.)
3. Huston, Wilber B., Rainey, A. Gerald, and Baker, Thomas F.: A Study of the Correlation Between Flight and Wind-Tunnel Buffeting Loads. NACA RM L55E16b, 1955.
4. Mayer, John P., and Valentine, George M.: Flight Measurements With the Douglas D-558-II (BuAero No. 37974) Research Airplane. Measurements of the Buffet Boundary and Peak Airplane Normal-Force Coefficients at Mach Numbers up to 0.90. NACA RM L50E31, 1950.
5. Baker, Thomas F.: Some Measurements of the Buffet Region of a Swept-Wing Research Airplane During Flights to Supersonic Mach Numbers. NACA RM L53D06, 1953.
6. Press, Harry, and Houbolt, John C.: Some Applications of Generalized Harmonic Analysis to Gust Loads on Airplanes. Jour. Aero. Sci., vol. 22, no. 1, Jan. 1955, pp. 17-26, 60.
7. Polentz, Perry P., Page, William A., and Levy, Lionel L., Jr.: The Unsteady Normal-Force Characteristics of Selected NACA Profiles at High Subsonic Mach Numbers. NACA RM A55C02, 1955.

Table I

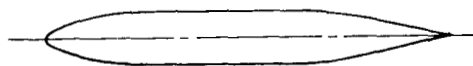
Store ordinates

(percent of store length)

Short-cylinder shape
(Stores A, B, C)



Long-cylinder shape
(Store D)

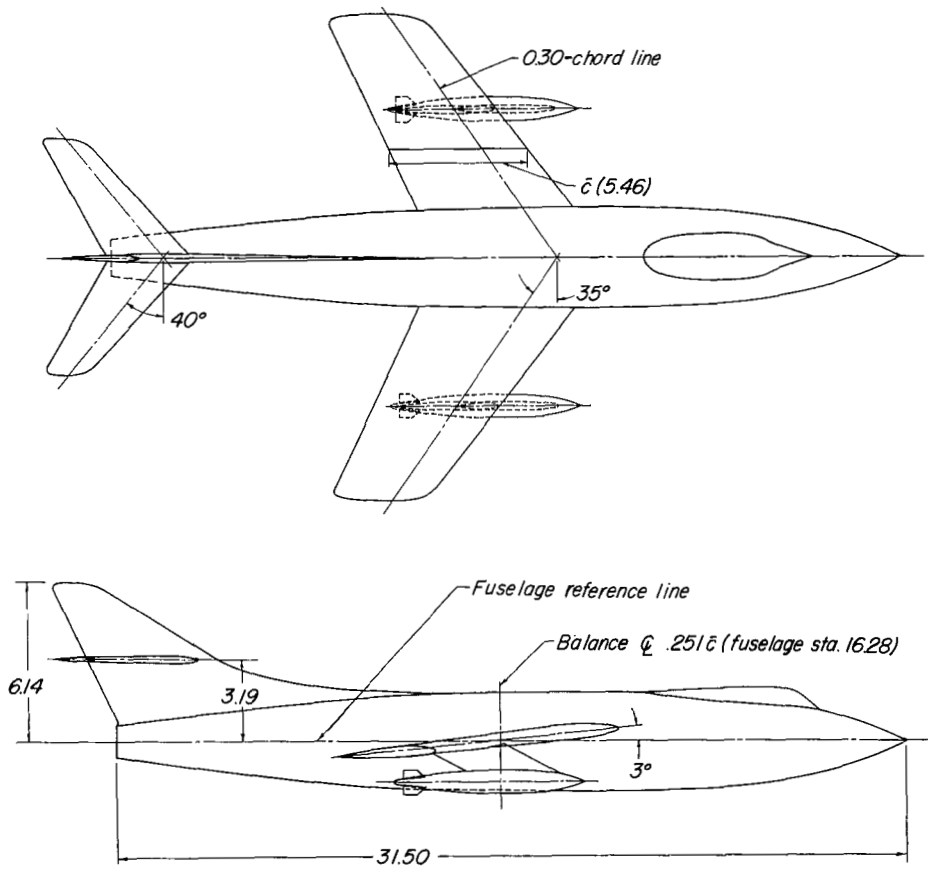


x	r
0	0
1.95	0.95
4.72	2.03
7.51	2.88
10.29	3.52
15.85	4.43
21.40	5.04
26.93	5.49
29.73	5.67
32.53	5.80
35.33	5.84
Straight line	
49.73	5.84
52.53	5.81
55.33	5.76
60.93	5.51
66.40	5.13
72.00	4.63
77.60	4.03
83.20	3.35
88.66	2.63
93.73	1.95
96.00	1.63
98.13	1.28
100.00	0
T.E.R.	0.56

x	r
0	0
1.11	1.88
2.23	2.62
3.35	3.17
4.47	3.63
5.57	4.01
6.71	4.35
8.93	4.84
14.49	5.79
17.28	6.07
20.08	6.28
21.43	6.37
23.37	6.40
25.69	6.44
Straight line	
61.47	6.44
63.60	6.40
64.80	6.37
67.07	6.28
70.00	6.07
72.67	5.79
78.40	4.85
79.20	4.72
Straight-line taper	
100.00	0

TABLE II
REPRESENTATIVE VALUES OF TEST CONDITIONS

M	p, lb/sq ft	q, lb/sq ft	T _t , °F	V, ft/sec	R
0.60	1,655	417	112	679	1.47×10^6
.70	1,523	522	125	791	1.57
.85	1,315	665	135	950	1.71
.90	1,247	707	138	1,000	1.75
.94	1,193	738	135	1,036	1.78
.96	1,166	753	128	1,048	1.81



Wing Geometry

Airfoil sections (normal to 0.30-chord line)

Root	NACA 63-010
Tip	NACA 63-010
Area, sq ft	0.684
Root chord, in.	6.78
Tip chord, in.	3.83
Aspect ratio	3.57
Taper ratio	0.565

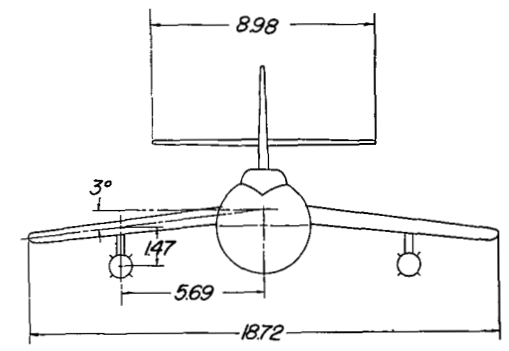
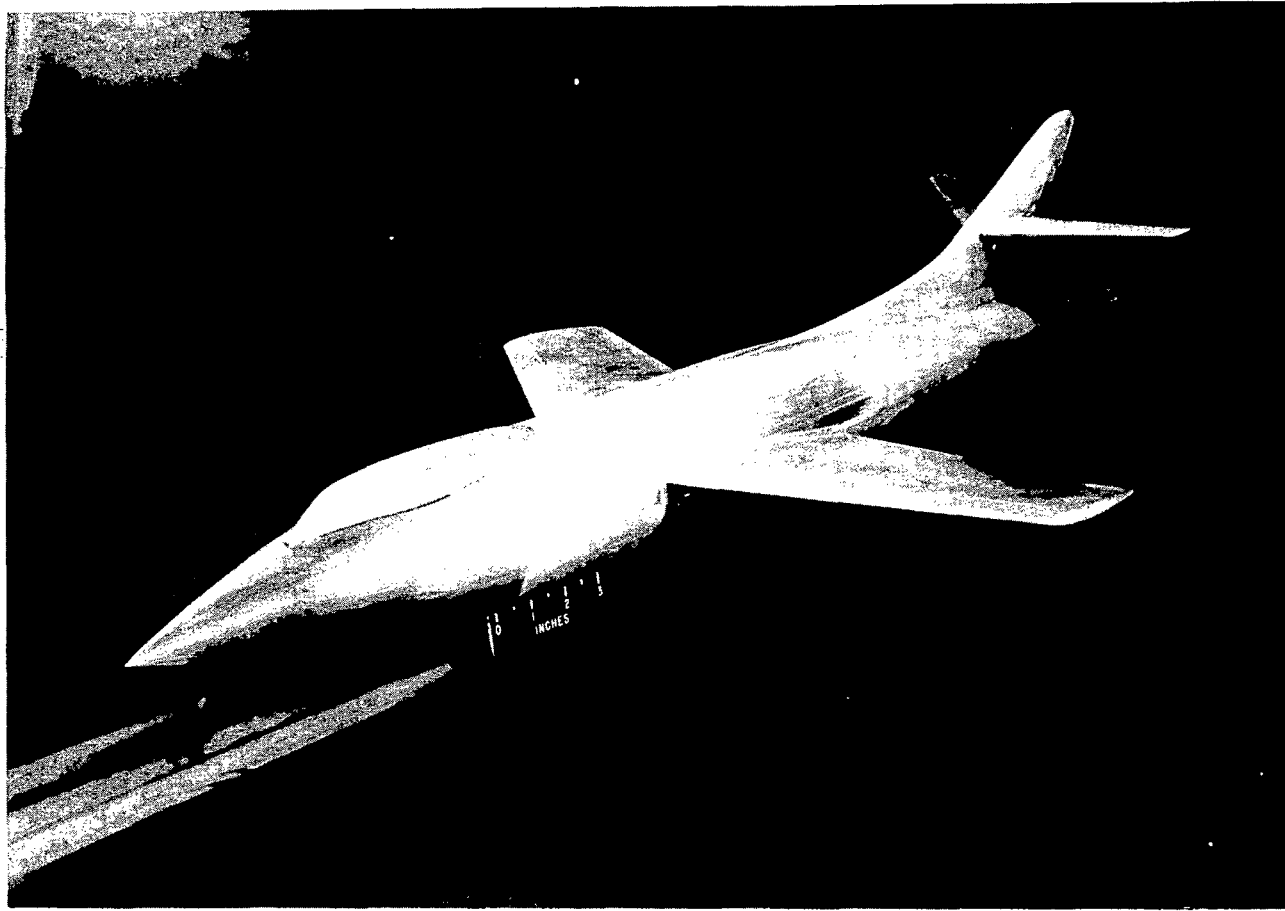


Figure 1.- Drawing of 1/16-scale model of the Douglas D-558-II airplane.
(All dimensions in inches.)



(a) Clean configuration.

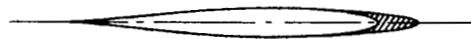
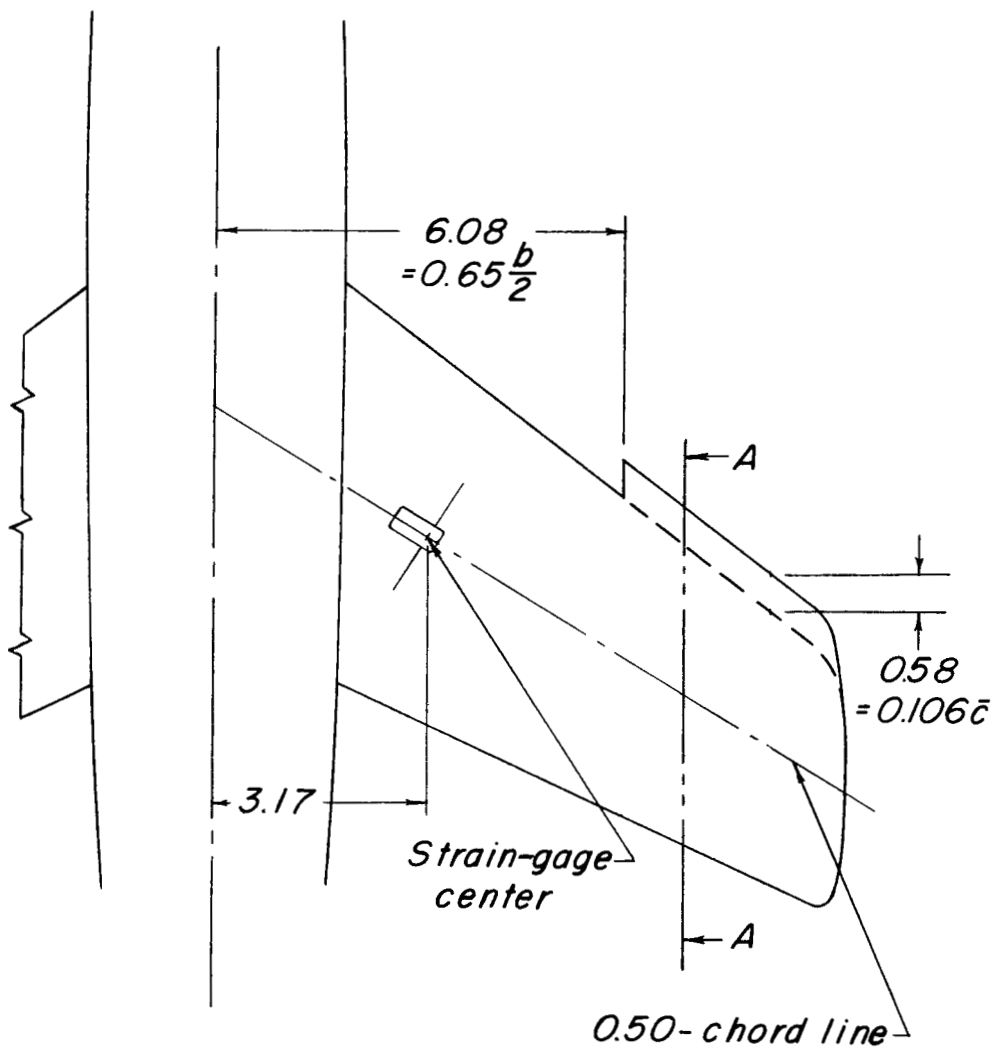
L-74746

Figure 2.- Photographs of 1/16-scale model of Douglas D-558-II research airplane in the Langley high-speed 7- by 10-foot tunnel.



(b) Model with store B and 7.6-percent-thick pylons. L-74749

Figure 2.- Concluded.



Section A-A

Figure 3.- Leading-edge chord-extensions and wing bending moment strain-gage installation.

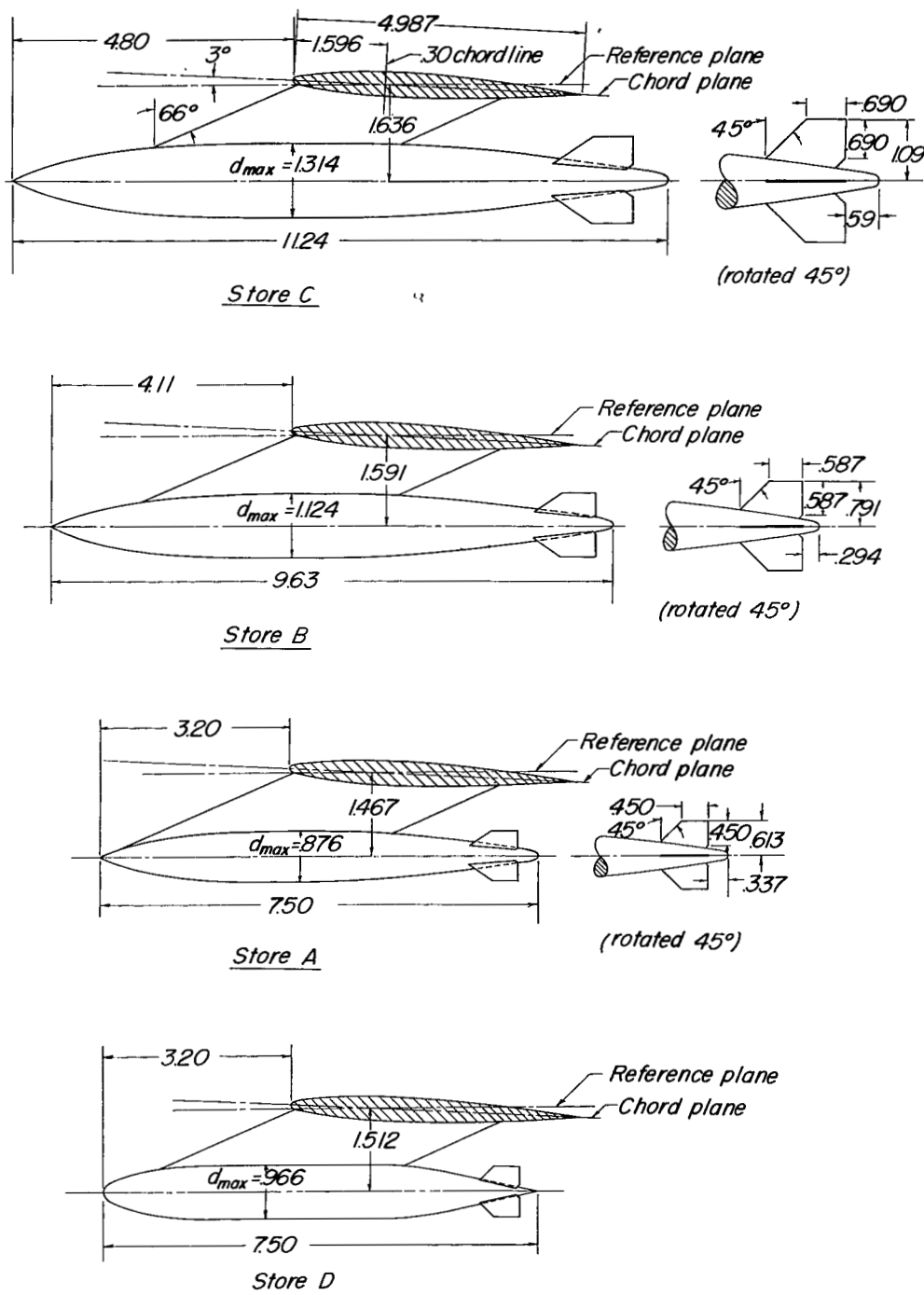
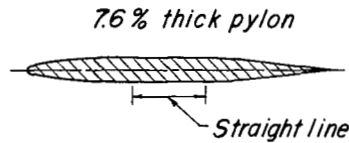
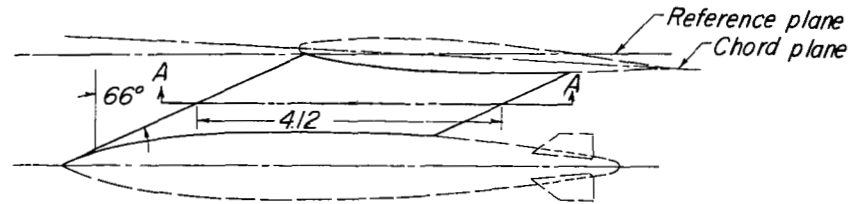
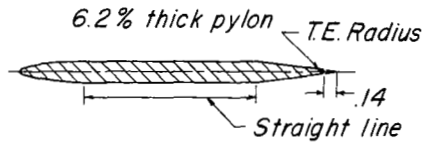


Figure 4.- Drawing of stores tested on 1/16-scale model of Douglas D-558-II airplane. (All dimensions in inches.)



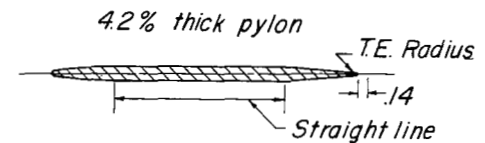
Section A-A

x	y	x	y
0	0	Straight line	
LER	.017	.241	.156
	.031	.256	.155
	.063	.272	.151
	.156	.288	.144
	.313	.303	.134
	.468	.319	.121
	.625	.334	.105
	.782	.366	.066
	.938	.397	.021
	1.195	.412	0
	1.250		.156
	1.407		.156



Section A-A

x	y
0	0
.200	.082
.400	.108
.600	.122
.852	.128
Straight line	
3.195	.128
4.260	0
4.120	T.E.R.=0.019



Section A-A

x	y
0	0
.200	.058
.400	.076
.600	.086
.852	.090
Straight line	
3.195	.090
4.260	0
4.120	T.E.R.=0.013

Figure 5.- Drawing of pylons tested on 1/16-scale model of Douglas D-558-II airplane. (All dimensions in inches.)

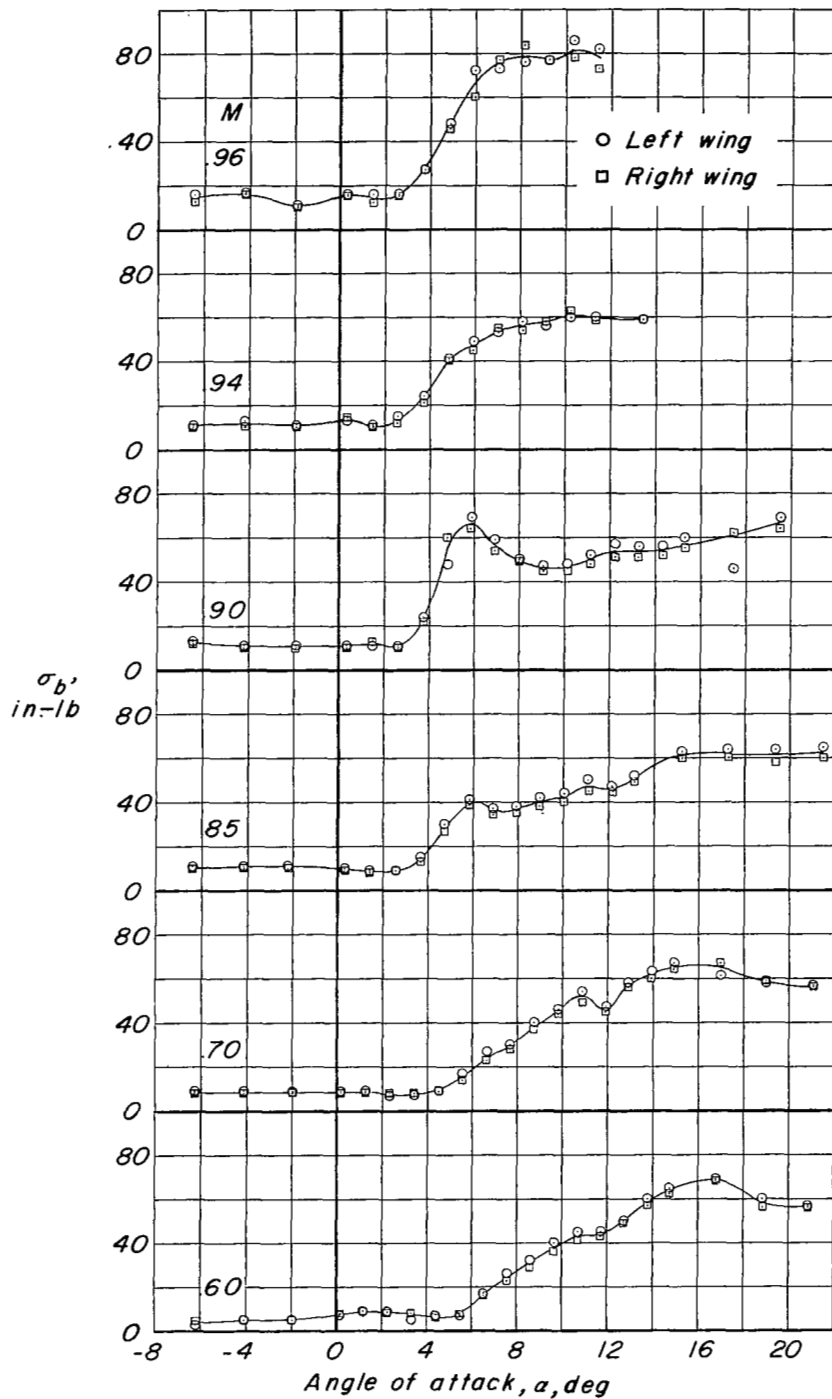


Figure 6.- Variation of fluctuations of wing bending moment with angle of attack. Clean configuration, $i_t = 0^\circ$.

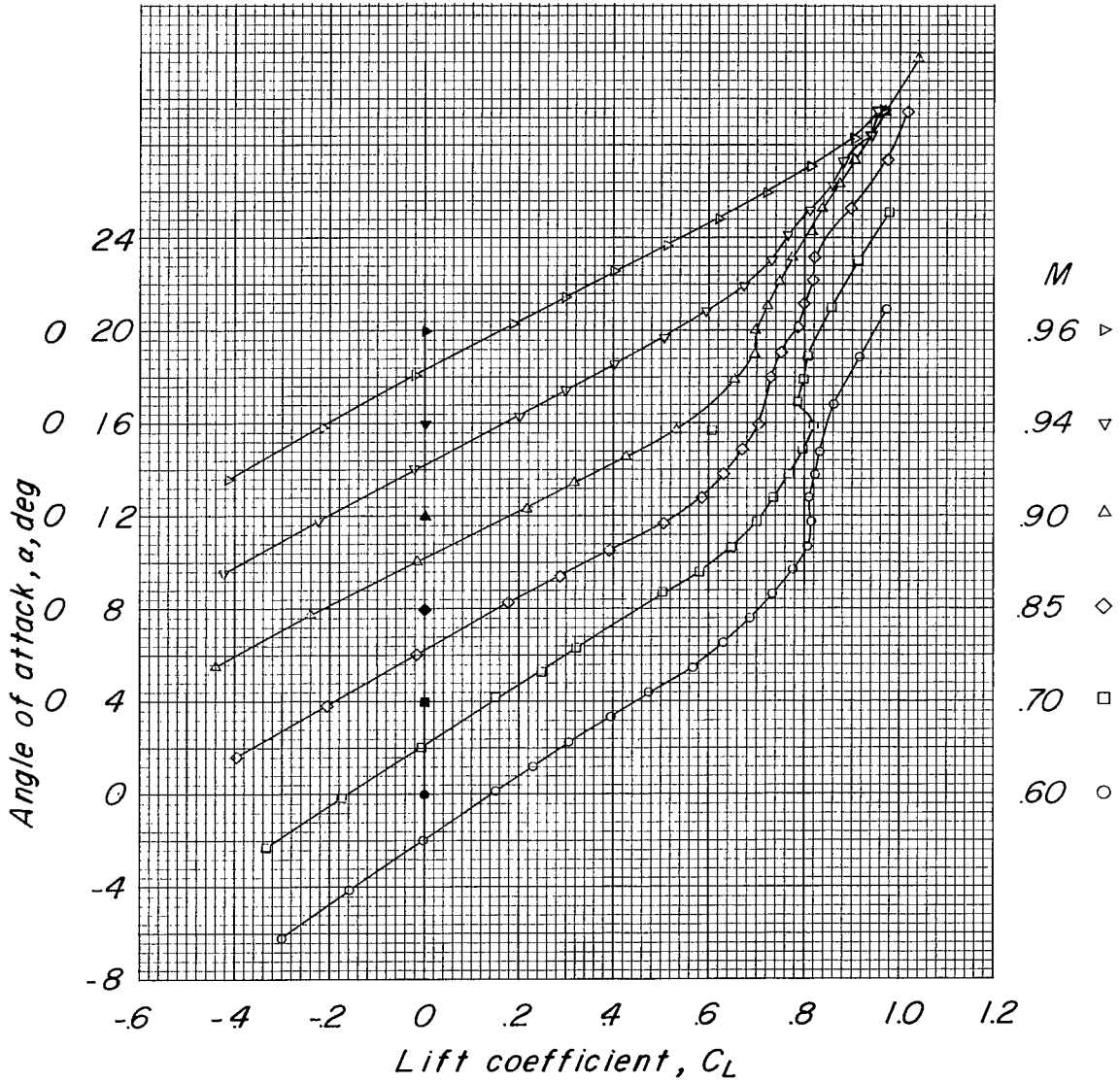


Figure 7.- Variation of lift coefficient with angle of attack. Clean configuration, $i_t = 0^\circ$. (Data from ref. 1.)

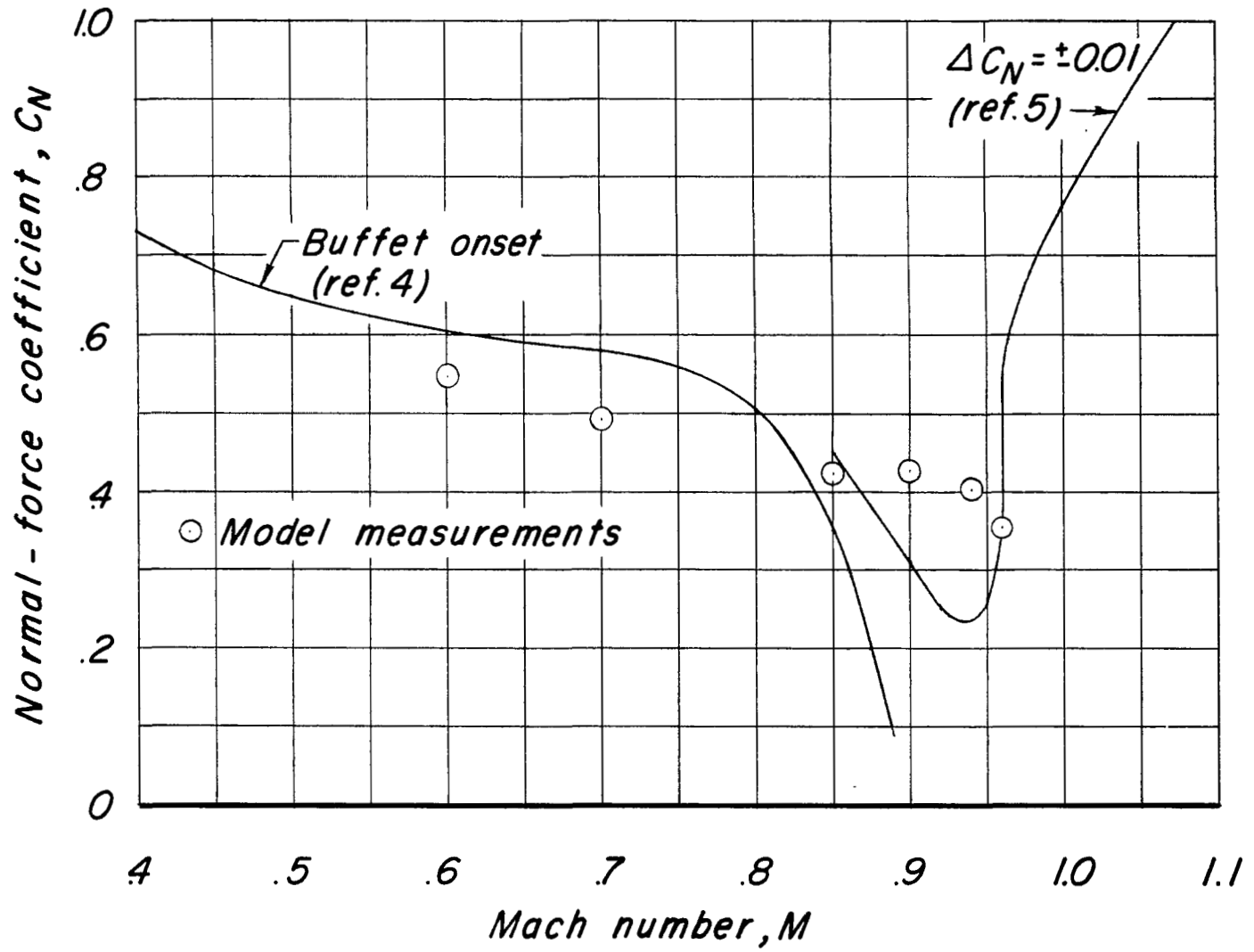


Figure 8.- Comparison of buffet boundaries determined in the wind tunnel and in flight.

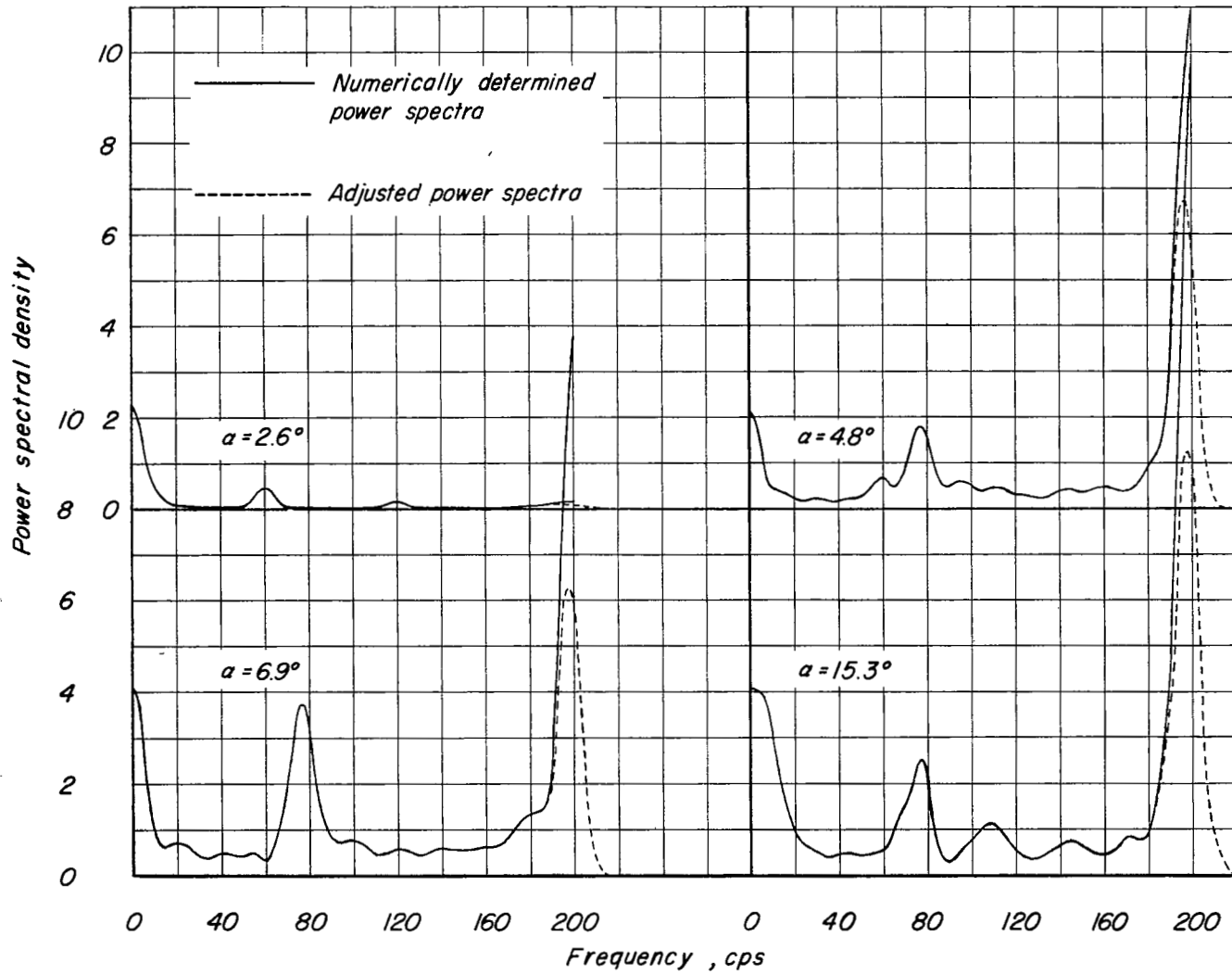


Figure 9.- Power spectra of wing bending moment. Clean configuration, $i_t = 0^\circ$, $M = 0.90$.

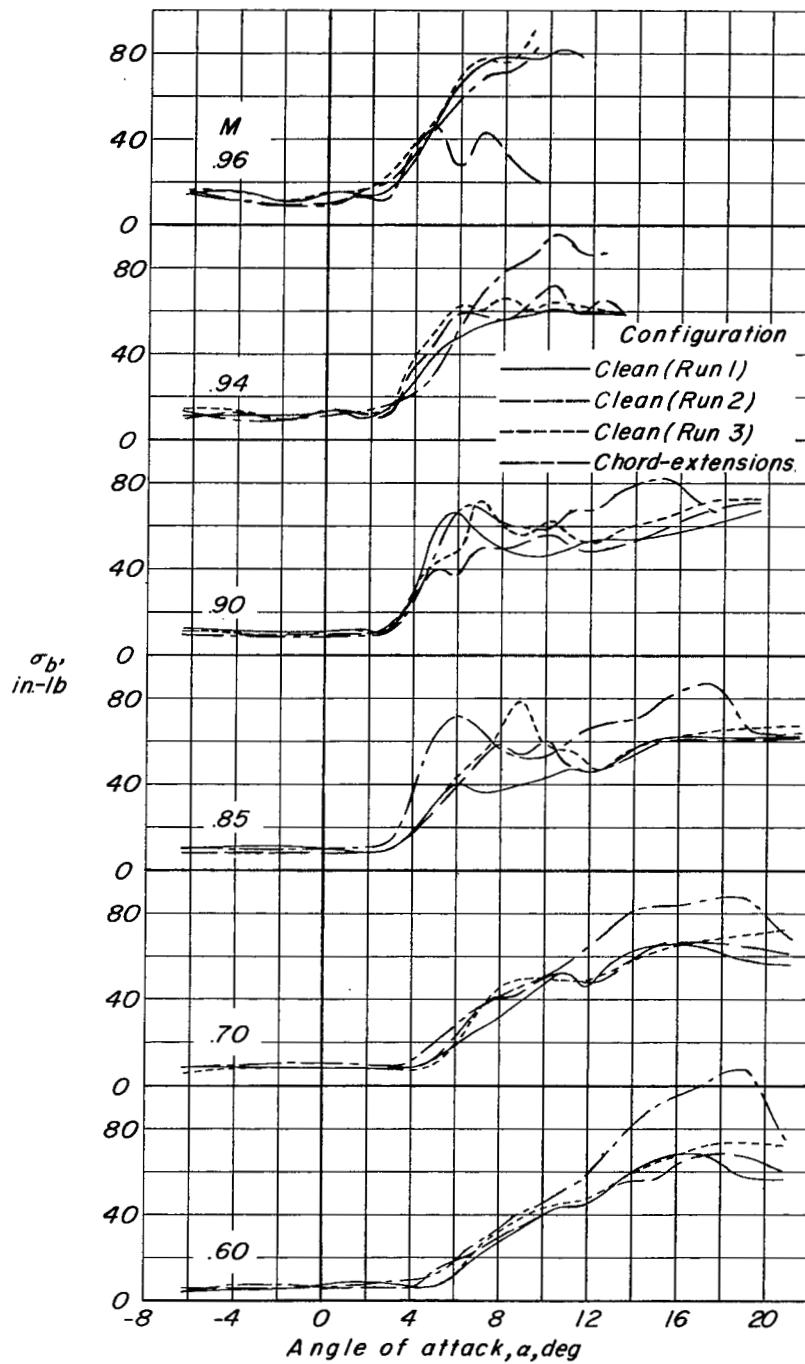
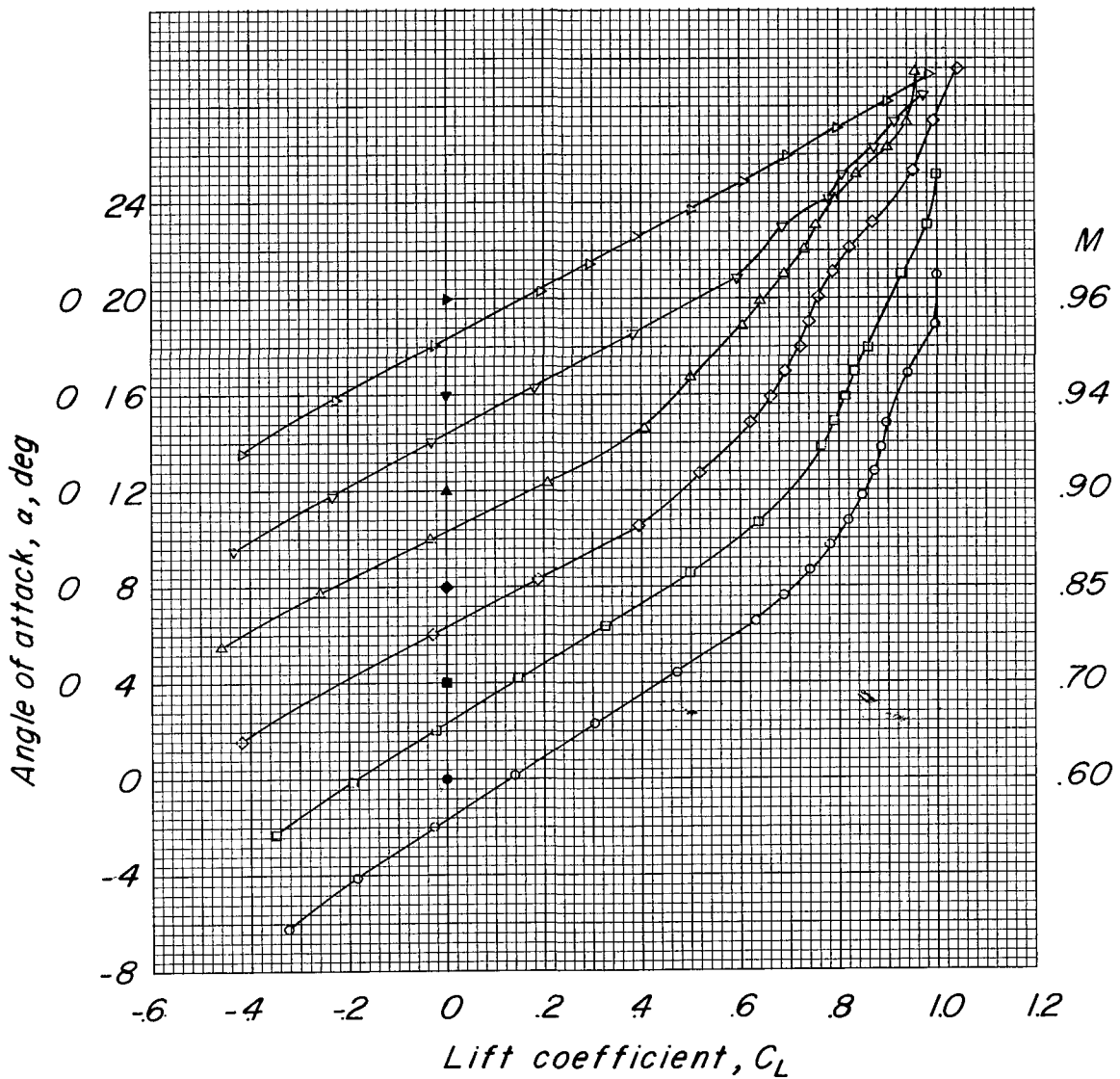
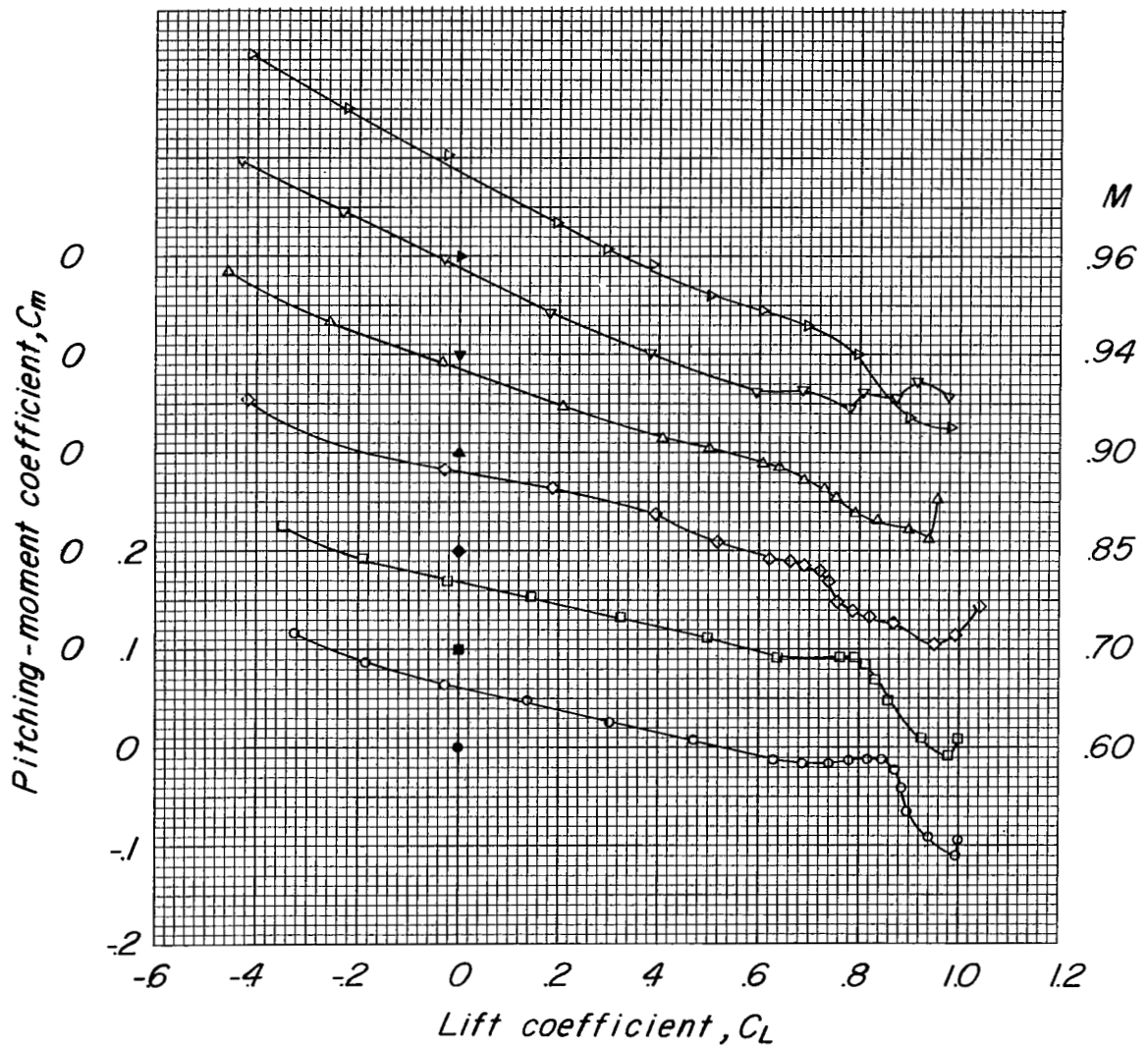


Figure 10.- Comparison of fluctuations of wing bending moment measured during three test runs in clean configuration and one test run with leading-edge chord-extensions. $i_t = 0^\circ$.



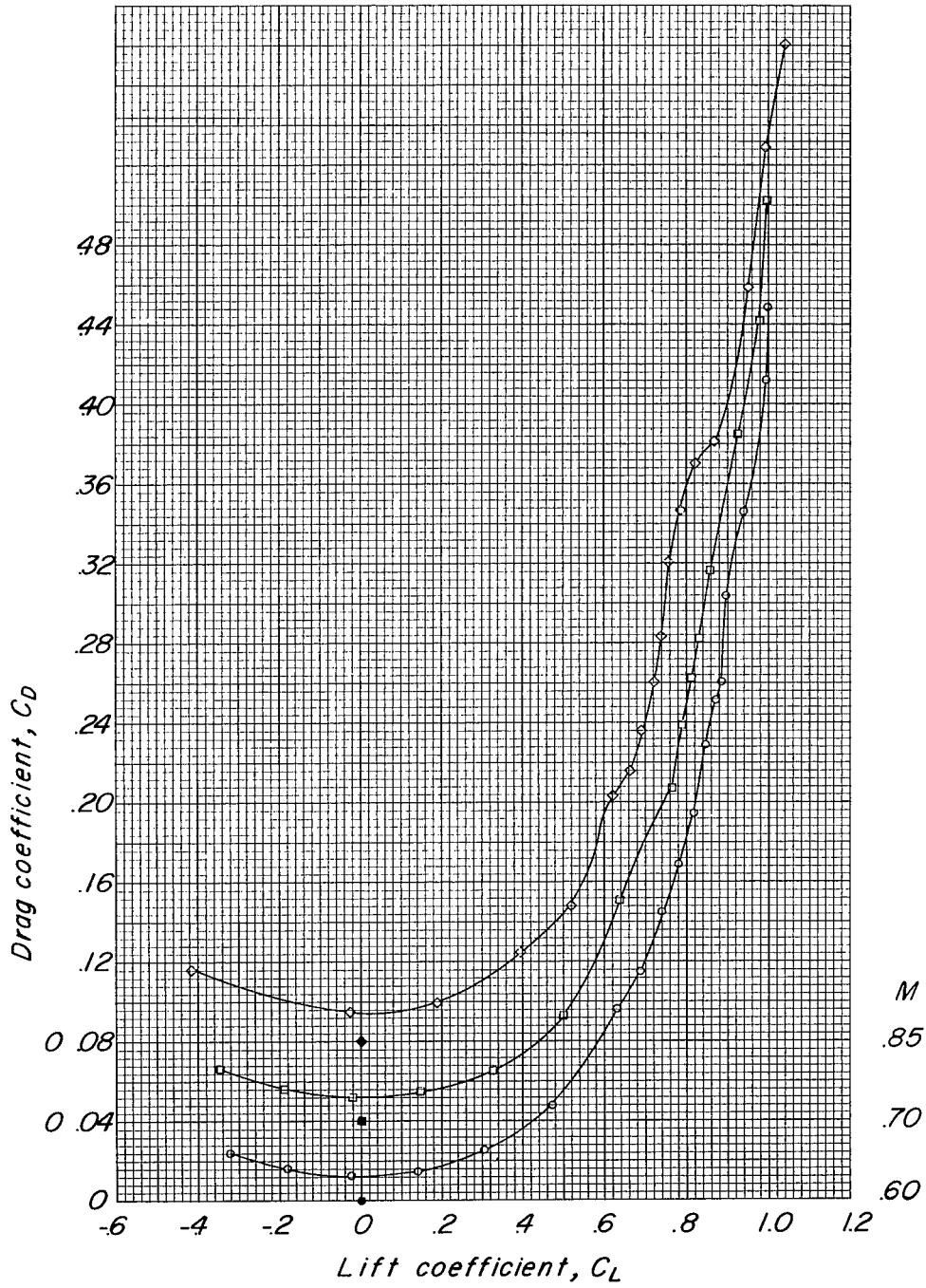
(a) α against C_L .

Figure 11.- Static aerodynamic characteristics of 1/16-scale model of Douglas D-558-II airplane with leading-edge chord-extensions. $i_t = 0^\circ$.



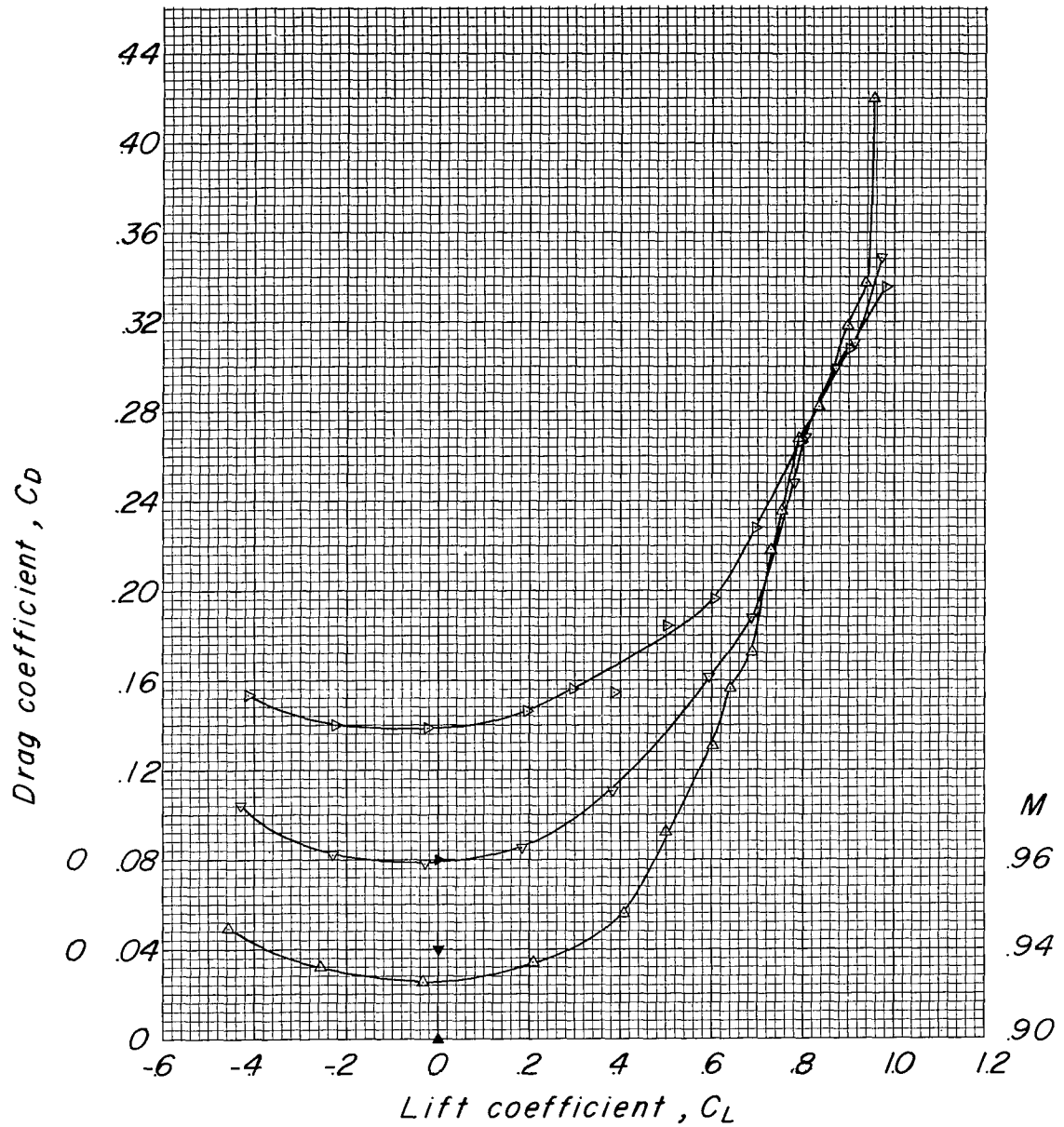
(b) C_m against C_L .

Figure 11.- Continued.



(c) C_D against C_L .

Figure 11.- Continued.



(c) Concluded.

Figure 11.- Concluded.

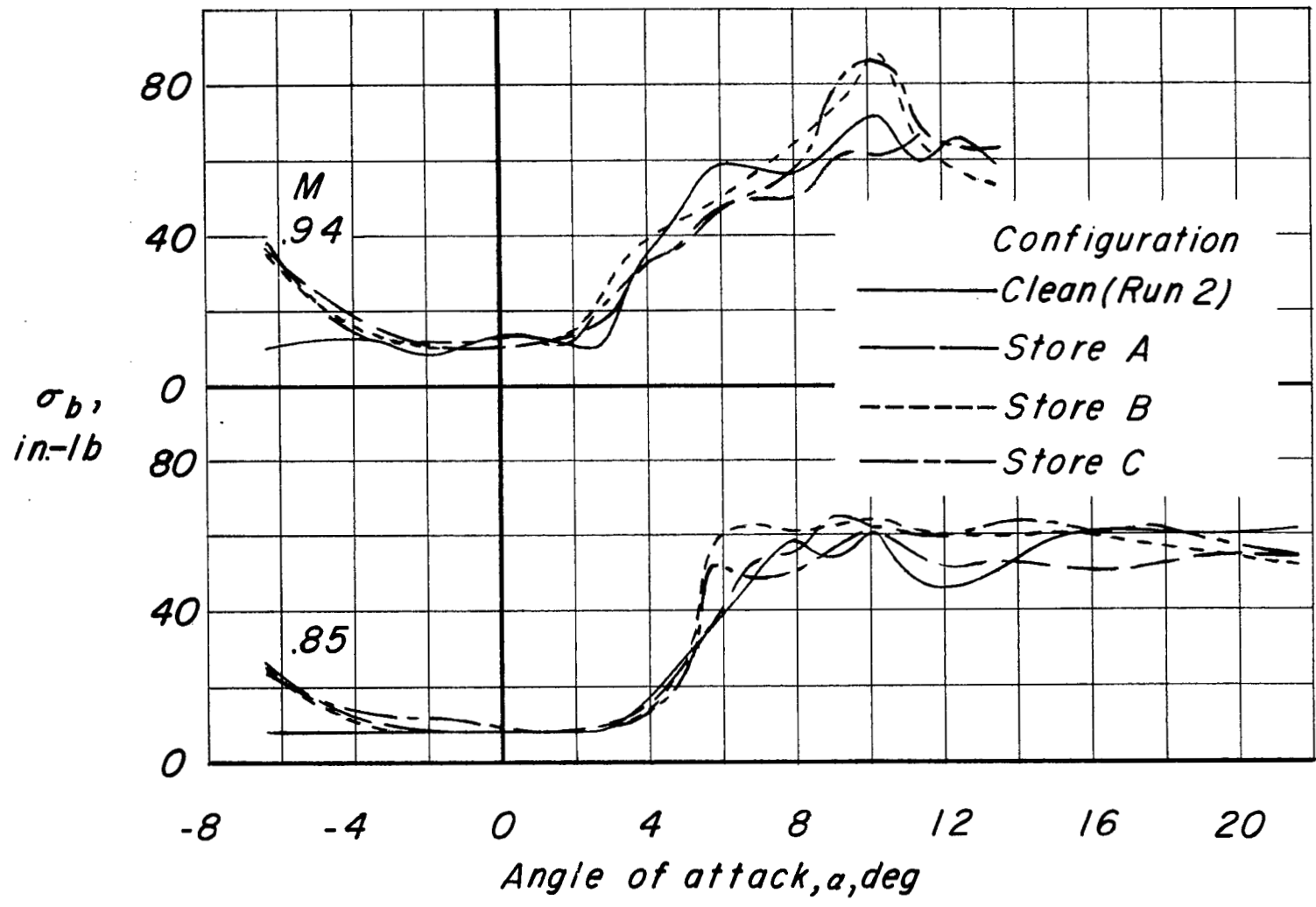


Figure 12.- Effect of store size on variation of fluctuations of wing bending moment with angle of attack. 7.6-percent-thick pylons, $i_t = 0^\circ$.

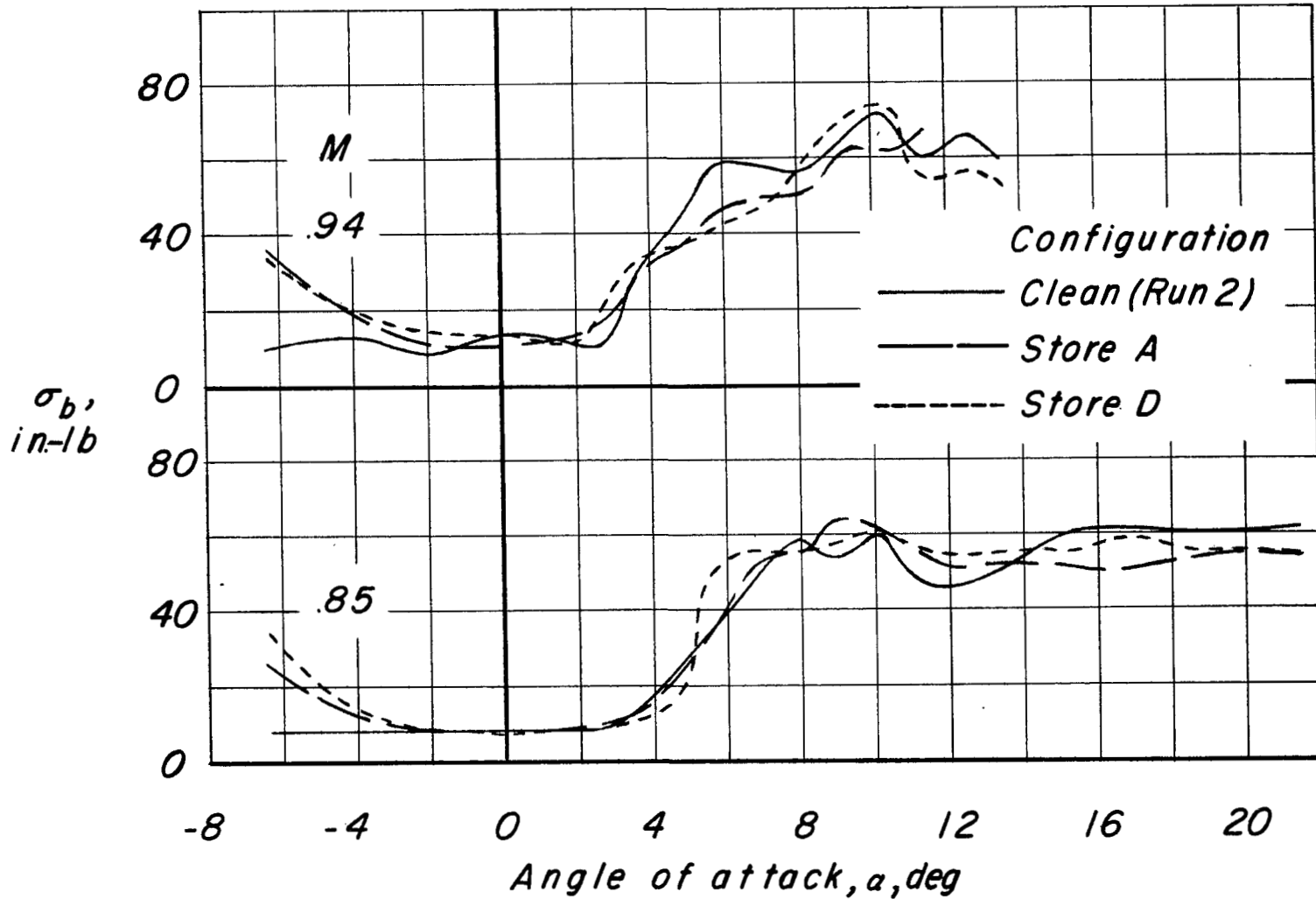


Figure 13.- Effect of store shape on variation of fluctuations of wing bending moment with angle of attack. 7.6-percent-thick pylons, $i_t = 0^\circ$.

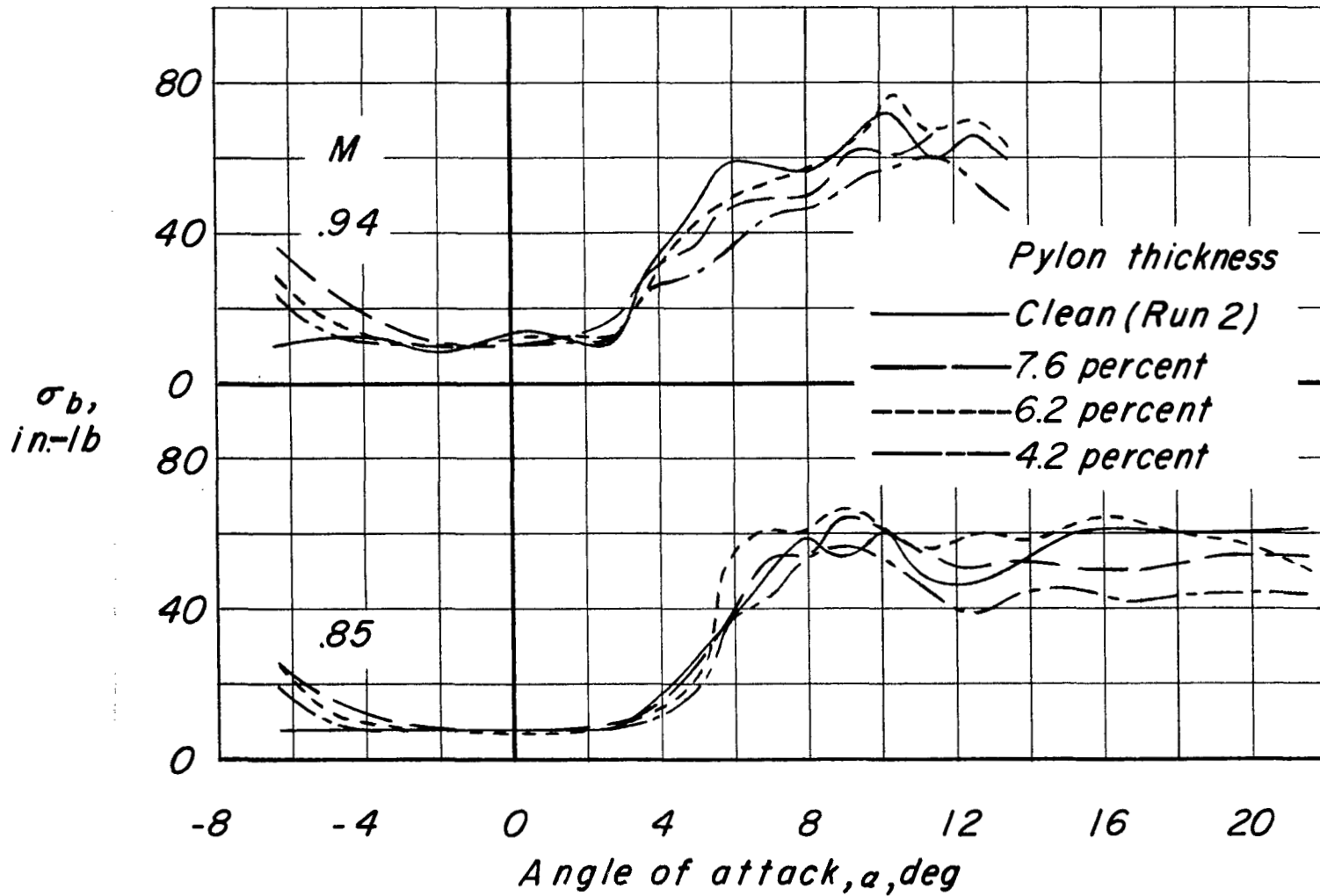


Figure 14.- Effect of pylon thickness on the variation of fluctuations of wing bending moment with angle of attack. Store A, $i_t = 0^\circ$.

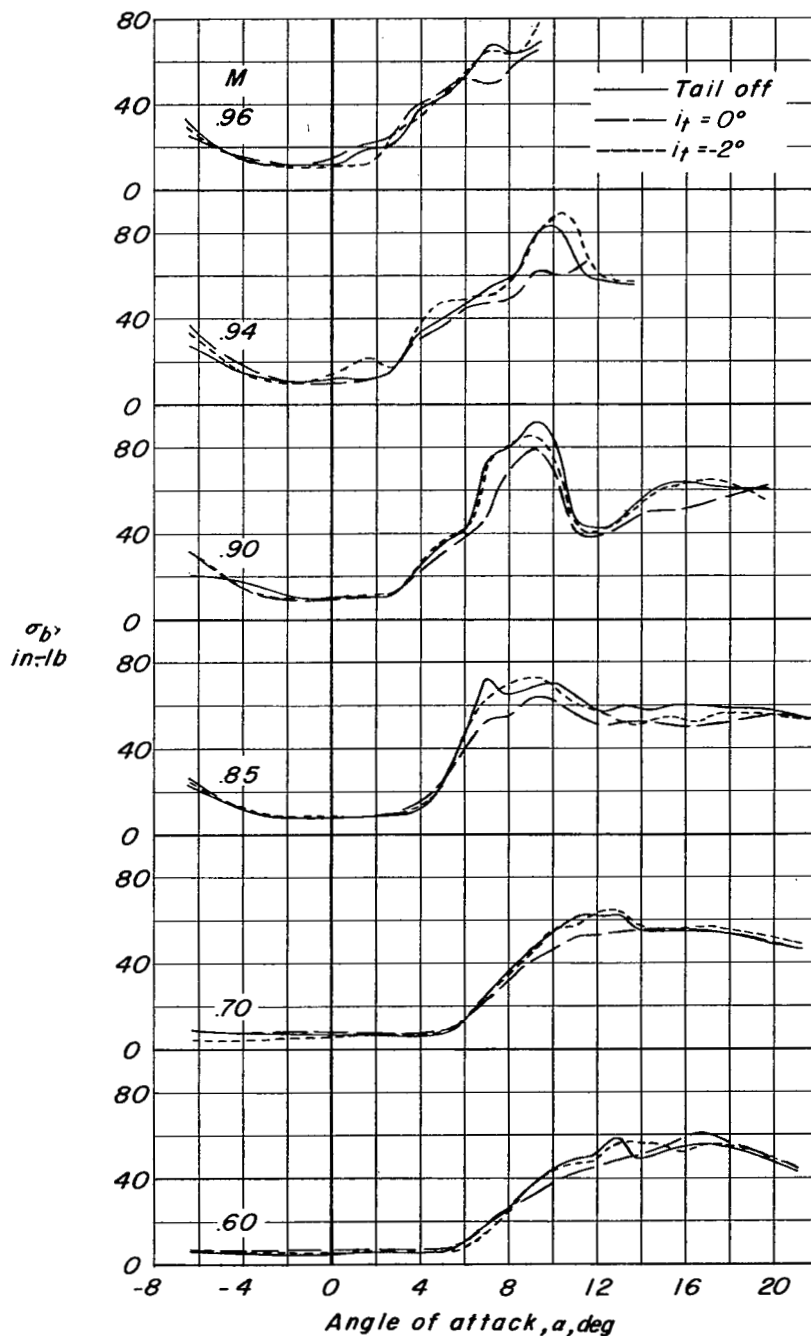


Figure 15.- Effect of horizontal tail on variation of fluctuations of wing bending moment with angle of attack. Store A and 7.6-percent-thick pylons.